Carbohydrate Polymers 198 (2018) 302–312

Contents lists available at ScienceDirect

Carbohydrate Polymers

journal homepage: www.elsevier.com/locate/carbpol

Rhizopus nigricans polysaccharide activated macrophages and suppressed tumor growth in CT26 tumor-bearing mice

Zhihong Wei[a,1], Guochuang Chen[b,d,*,1], Pengying Zhang[b], Lei Zhu[c], Linan Zhang[e], Kaoshan Chen[b,c,*]

[a] Gynecology Department, First Affiliated Hospital of Shenzhen University, Shenzhen Second People's Hospital, Shenzhen, China
[b] School of Life Science and National Glycoengineering Research Center, Shandong University, Jinan, China
[c] Anhui Provincial Engineering Research Center for Polysaccharide Drugs, Anhui Province Key Laboratory of Active Biological Macro-molecules, School of Pharmacy, Wannan Medical College, Wuhu, China
[d] Institute of Biomedicine and Biotechnology, Shenzhen Institutes of Advanced Technology, Chinese Academy of Sciences, Shenzhen, China
[e] Second Affiliated Hospital of China Medical University, Shenyang, China

ARTICLE INFO

Keywords:
Polysaccharides
Rhizopus nigricans
Macrophage
Antitumor
CT26 colon cancer

ABSTRACT

In this study, a homogeneous polysaccharide (RPS-1) was extracted from liquid-cultured mycelia of *Rhizopus nigricans*. The weight-average molecular weight of RPS-1 was 1.617×10^7 g/mol and structural characterization indicated that RPS-1 was a non-starch glucan which consisted of a backbone structure of (1→4)-linked α-D-glucopyranosyl residues substituted at the O-6 position with α-D-glucopyranosyl branches. RPS-1 stimulated the production of nitric oxide and tumor necrosis factor-α by triggering phosphorylation of mitogen-activated protein kinases and nuclear translocation of nuclear factor kappa B p65 in RAW 264.7 macrophage cells. Moreover, intragastric administration of RPS-1 improved the immune function of CT26 tumor-bearing mice and significantly inhibited the growth of transplanted tumor. In combination with 5-FU, RPS-1 enhanced antitumor activity of 5-FU and alleviated its toxicity on immune system. These findings suggested that RPS-1 has the potential for the development of functional foods and dietary supplements.

1. Introduction

Fungal polysaccharides have long been appreciated for their biological and pharmacological activities, including immunomodulatory, antitumor, antioxidant, antiviral and anti-infection (Wasser, 2010; Yu, Shen, Song, & Xie, 2018). A wide range of fungal glucans showed immunomodulatory and antitumor activities have been obtained from fruit bodies, mycelia and liquid culture broth. These glucans present diverse structures with (1→3)-, (1→4)- and/or (1→6)-linked linear or branched α-glucans, β-glucans and mixed α/β-glucans, and molecular weight ranged from thousands to millions Da (Synytsya & Novak, 2013). As the most studied fungal glucan, β-glucans are considered as potent immunomodulators and responsible for the beneficial effects in the outcome of malignant tumor (Ina, Kataoka, & Ando, 2013; Namikawa et al., 2015). Upon specific interactions with several cell surface receptors, such as toll-like receptor, complement receptor 3 and dectin-1, β-glucans can trigger a wide spectrum of immune responses through various signaling pathway (Brown & Gordon, 2001; Gantner, Simmons, Canavera, Akira, & Underhill, 2003; Thornton, Vetvicka, Pitman, Goldman, & Ross, 1996).

Despite the well documented β-glucans, little is known about the immunoregulatory activities of fungus derived α-(1→4)-glucans and their underlying mechanisms. Macrophages are one of the major types of phagocytes and play vital roles in innate and adaptive immune system. More important, macrophages orchestrate immune response against cancer by phagocytosing aberrant cells, presenting tumor antigens and secreting heterologous proinflammatory cytokines (Long & Beatty, 2013). Recently research reported that maitake α-(1→4)-glucans served as biological response modifiers with the capability to activate macrophages and dendritic cells and inhibited tumor growth in vivo (Masuda, Nakayama, Tanaka, Naito, & Konishi, 2017; Sun et al., 2016; Wang et al., 2017). YCP, a homogeneous α-(1→6)-branched α-(1→4)-glucan purified from the mycelium of marine fungus, was found to be able to increase phagocytic activity in mice and stimulate NO

Abbreviations: MAPKs, mitogen-activated protein kinases; NF-κB, nuclear factor-κB; NO, nitric oxide; HPSEC-MALLS, high performance size-exclusion chromatography with multiangle laser light scattering; PMB, polymyxin B; 5-FU, 5-fluorouracil

* Corresponding authors. Postal address: School of Life Science and National Glycoengineering Research Center, Shandong University, No. 27 South Shanda Road, Jinan, China.
E-mail addresses: chenguochuang@126.com (G. Chen), ksc313@126.com (K. Chen).

[1] These authors contributed equally to this work, thus share the first authorship.

https://doi.org/10.1016/j.carbpol.2018.06.076
Received 22 March 2018; Received in revised form 15 June 2018; Accepted 15 June 2018
Available online 18 June 2018
0144-8617/

release in macrophages through p38 signaling axis (Chen et al., 2009; Yang et al., 2005). Macrophage activation may partially underlie immunoregulatory and antitumor activities of α-(1→4)-glucans.

Rhizopus nigricans is a zygomycete filamentous fungus and widely used in food and pharmaceutical industry. In this study, we obtained a novel bioactive glucan from liquid-cultured mycelia of *R. nigricans* and explored the underlying molecular mechanisms of macrophage activation. The antitumor effects of *R. nigricans* polysaccharide were further investigated in CT26 colon cancer-bearing mice.

2. Materials and methods

2.1. Materials

DEAE sepharose Fast Flow and Sephacryl S-500 HR were obtained from General Electric Healthcare Life Sciences (Pittsburgh, USA). Fetal bovine serum, dulbecco's modified eagle medium (DMEM), Lipofectamine® 2000, penicillin and streptomycin were provided by Thermo Fisher Scientific (Waltham, USA). Monosaccharides, lipopolysaccharide (LPS), 4′,6-Diamidino-2-phenylindole dihydrochloride (DAPI), polymyxin B (PMB) and 5-fluorouracil (5-FU) were purchased from Sigma-Aldrich (St. Louis, USA). 1-Phenyl-3-methyl-5-pyrazolone (PMP) was obtained from Acros Organics (Geel, Belgium). Antibodies against IκB-α, NF-κB p65 (RelA), JNK1/2, phospho-JNK1/2, and β-actin were purchased from Santa Cruz Biotechnology (Dallas, USA). Antibodies against p38, phospho-p38, p44/42 (ERK1/2), phospho-p44/42 (ERK1/2), and histone H2A were provided by Cell Signaling Technology (Danvers, USA). The cell lysis buffer, nuclear and cytoplasmic protein extraction kit, NF-κB nuclear translocation assay kit and horseradish peroxidase (HRP)-labeled second antibodies were supplied by Beyotime Institute of Biotechnology (Shanghai, China). The pNL3.2.NF-κB-RE and pRL-TK plasmids and dual-luciferase® reporter assay system were obtained from Promega (Beijing, China). Mouse TNF-α and interleukin-2 (IL-2) ELISA kits were purchased from RayBiotech (Norcross, USA).

2.2. Organism and growth conditions

R. nigricans was preserved in Laboratory of Biomass Resources, Shandong University (Jinan, China). The strain was cultured in shaking flask containing potato dextrose broth under controlled conditions (28 °C, 130 rpm) for 10 days.

2.3. Extraction and purification of the R. nigricans polysaccharides

Liquid-cultured mycelia of *R. nigricans* were extracted in boiling water for 2 h and the extract was treated with 3 volumes of ethanol at 4 °C overnight. The precipitate was dissolved in distilled water and deproteinated according to the method of Sevag (Sevag, 1938). The resulted polysaccharide solution was decolorized with D301R resin, followed by dialyzed and lyophilized to obtain the crude polysaccharides. The crude polysaccharides were loaded into DEAE Sepharose Fast Flow column (1.6 cm × 20 cm) and eluted with a linear gradient of sodium chloride solution (0–0.5 M). The unabsorbed fraction was collected and further purified using Sephacryl S-500 HR column (1.6 cm × 60 cm) and the fraction of major peak was collected and lyophilized to powder, named as RPS-1. The total sugar content of RPS-1 was measured by phenol-sulfuric acid method and glucose was used as standard. The endotoxin contamination was tested by the Limulus amoebocyte lysate assay, showing negative value.

2.4. Homogeneity, molecular weight and root mean square radius

The purity, molecular weight (M_w) and root mean square (RMS) radius of RPS-1 were determined by using high performance size-exclusion chromatography coupled with multiangle laser light scattering (HPSEC-MALLS). HPSEC-MALLS measurements were performed on a Waters 2695 instrument (Waters, USA) equipped with OHpak SB-806M (Shodex, Japan) at 25 °C. RPS-1 was dissolved in distilled water and incubated for 3 h. All the solutions were purified by a 0.45 μm filter. The elution was maintained at a flow rate of 0.5 ml/min and monitored by Optilab T-rEX differential refractive index detector (Wyatt, USA) and multiangle laser light scattering instrument equipped with DAWN HELEOS II light scattering (Wyatt, USA) at angles of 35°, 43°, 52°, 60°, 69°, 80°, 90°, 100°, 111°, 121°, 132°, 142°, and 152°. The Astra software was utilized for data acquisition and analysis.

2.5. Monosaccharide composition analysis

Monosaccharide analysis was performed as described previously (Chen et al., 2013).

2.6. Methylation analysis

Methylation of RPS-1 was performed as previous described (Ciucanu & Kerek, 1984). The resulting methylated product was hydrolyzed with 2 M TFA at 120 °C for 2 h followed by reduction with $NaBD_4$ and acetylation with acetic anhydride to yield partially methylated alditol acetates which were further quantified by gas chromatograph-mass spectrometer (GC–MS) using a HP-5 MS fused silica capillary column (30 m × 0.25 mm i.d., 0.25 μm, Agillent, USA). The column temperature was set at 120 °C when injected, then increased to 200 °C at 4 °C/min, then to 280 °C at 10 °C/min, and kept at 280 °C for 5 min. Helium was used as the carrier gas.

2.7. Nuclear magnetic resonance analysis

A total of 10 mg of RPS-1 was dissolved in 0.5 ml of D_2O. The ^1H and ^{13}C NMR spectra were recorded on a Bruker AVANCE-300 MHz NMR spectrometer (Bruker, Germany) at 25 °C.

2.8. Cells and animals

Murine macrophage cell line RAW 264.7 and CT26 mouse colon cell line were purchased from the Cell Bank of Type Culture Collection of Chinese Academy of Sciences (Shanghai, China). Cells were maintained in DMEM supplemented with 10% fetal bovine serum, 100 IU/ml penicillin and 100 μg/ml streptomycin. Cell cultures were incubated in humidified atmosphere of 5% CO_2 at 37 °C. Female BALB/c mice weighing 18–22 g were purchased from Nanjing Qinglong mountain farm (Nanjing, China) and acclimatized for 1 week before used. All the animals were kept according to the National Institute of Health Guide for the Care and Use of Laboratory Animals, and all experimental protocols were in accordance with the institutional guidelines of the Animal Care and Use Committee at Shandong University.

2.9. Measurement of NO and TNF-α

Logarithmically growing RAW 264.7 cells were placed in 96-well plate and treated by a series of concentrations of RPS-1 for 24 h. LPS (100 ng/ml) was used as positive control. After treatment, the levels of NO and TNF-α were assayed by Griess reagent and enzyme-linked immunosorbent assay kit according to the manufacturer's protocols, respectively.

2.10. Immunofluorescence staining

RAW 264.7 cells were plated in 6-well plate and exposed to RPS-1 (400 μg/ml) or LPS (100 ng/ml) for 30 min. After treatment, cells were rinsed with cold phosphate buffer solution (PBS), fixed by paraformaldehyde and incubated with primary antibody against NF-κB p65 overnight at 4 °C overnight. And then cells were incubation with a Cy-3

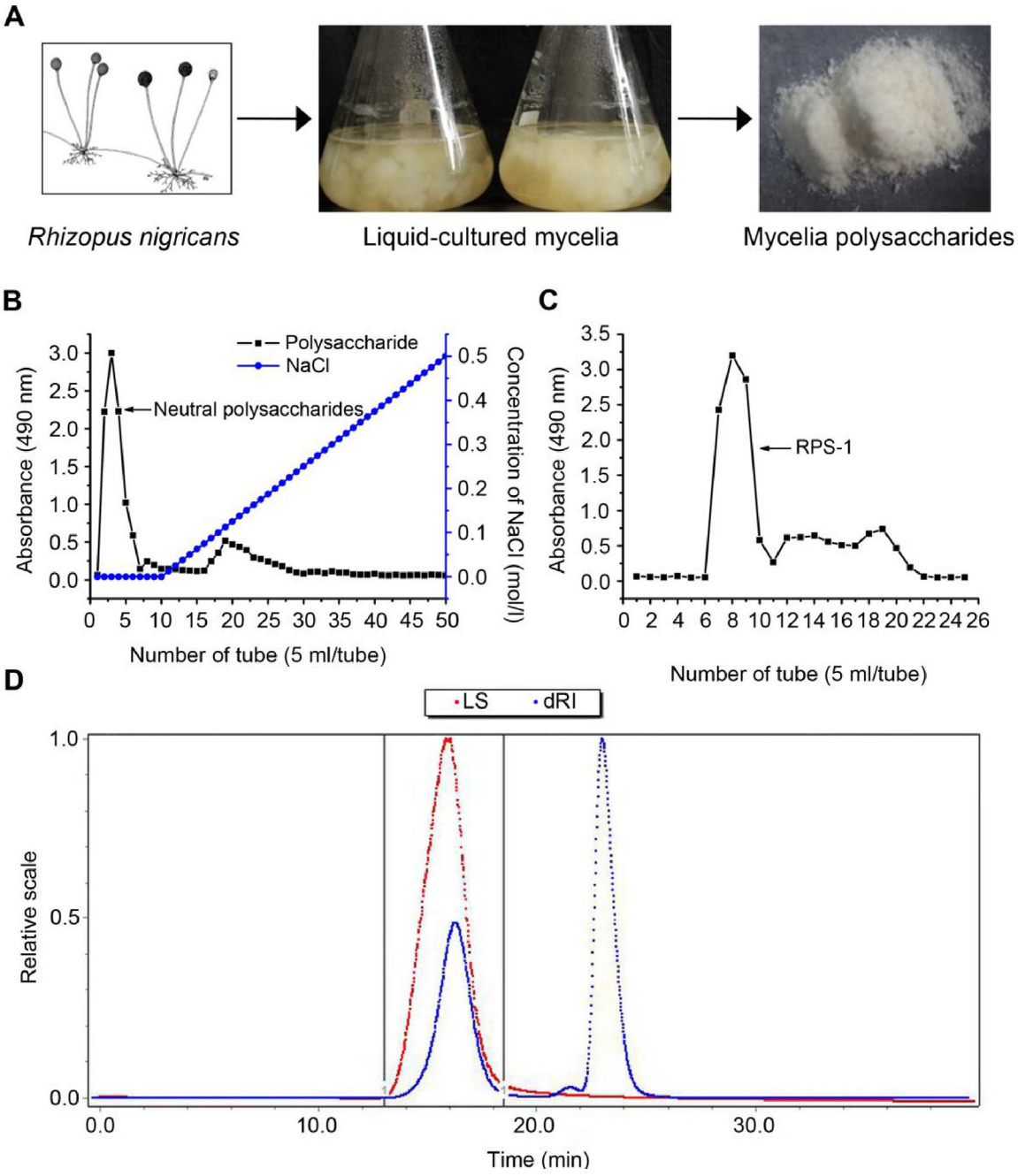

Fig. 1. Separation and purification of *R. nigricans* polysaccharides. (A) The crude *R. nigricans* polysaccharides were extracted from liquid cultivated mycelium and separated by (B) DEAE-Sepharose Fast Flow column and (C) Sephacryl S-500 HR. (D) The homogeneity of RPS-1 was analyzed by HPSEC-MALLS. LS: light scattering detector, dRI: differential refractive index detector.

conjugated secondary antibody for 1 h at room temperature and stained with DAPI for 5 min. The prepared samples were photographed by using fluorescence microscopy (Olympus, Japan).

2.11. Western blot

RAW 264.7 cells were treated with RPS-1 or LPS for indicated time and cell lysates were centrifuged at 12,000 × *g* for 15 min at 4 °C to remove cellular debris. The protein concentrations were determined using BCA method. For the extraction of nuclear and cytoplasmic protein, a commercially available kit (Beyotime, China) was used according to the manufacturer's protocols. The protein samples were mixed with SDS-PAGE loading buffer and boiled at 100 °C for 5 min. The samples containing equal amounts of protein were separated by 10–12% SDS–PAGE and then transferred onto polyvinylidene fluoride member (Millipore, USA). The membrane was blocked with solution containing 5% skim milk in Tris-buffered saline with 0.1% Tween-20 (TBST) for 2 h at room temperature, and incubated with primary antibodies at 4 °C overnight. The blots were washed 3 times with TBST and further probed with HRP-conjugated secondary antibodies for 1 h at room temperature. The visualization of the immune complexes was performed using an enhanced chemiluminescence detection system.

2.12. Dual-luciferase reporter assay

The plasmids used for transfection were purified by using an E.Z.N.A.® Endo Free Plasmid Mini Kit (Omega, USA). Transfection was performed by using the Lipofectamine® 2000 according to the

manufacturer's recommendations. Briefly, the transfection mixture consisted of 500 ng of reporter plasmid and 2 μl of transfection reagent was added dropwise to each well and incubated for 6 h. The culture was replaced with DMEM supplemented with 10% fetal bovine serum and incubated for 12 h. After transfection, the cells were treated with RPS-1 or LPS for 12 h and the transcriptional activity of NF-κB was detected by dual-luciferase reporter assay system. The results were recorded with a Glomax® 96 microplate luminometer (Promega, USA).

2.13. In vivo model to assess anti-tumor effects of R. nigricans polysaccharides

Model of subcutaneously transplanted tumor was established by inoculating 0.2 ml of CT26 cell suspension (3×10^6 cells/ml) into the right axillary region of mouse. After 24 h, the mice were randomly divided into six groups (six mice in each group) and received intragastric administration of RPS-1 or 5-FU for 10 days. The three groups of mice received administration of RPS-1 at different dosages (50, 100 and 200 mg/kg/day), respectively. The positive control group was treated with 5-FU (20 mg/kg/day), and the control group was administered 0.9% saline solution. In the combination group, RPS-1 (200 mg/kg/day) was applied in combination with 5-FU (20 mg/kg/day). The animals were sacrificed when intervention caused mouse weight loss of 30% or more. Thymus and spleen indexes were calculated as the weight of thymus and spleen relative to body weight: organ index (mg/g) = W_{organ}/W_{body}, where W_{organ} and W_{body} were the weight of the organ and body weight of mice, respectively. The tumor inhibitory rate was calculated by following formula: tumor inhibitory rate (%) = $(W_{control}-W_{treated})/W_{control} \times 100\%$, where $W_{treated}$ and $W_{control}$ were the average tumor weight of the treated and control group, respectively.

2.14. Statistical analysis

All data were analyzed using one-way ANOVA using SPSS13.0 software and presented as the mean ± standard deviation (SD). $^*P$ values of less than 0.05 were considered statistically significant.

3. Results

3.1. Isolation and purification of RPS-1

The crude polysaccharides from liquid-cultured mycelia of *R. nigricans* were obtained by hot water extraction, ethanol precipitation, deproteinization and decoloration (Fig. 1A). After separation by DEAE Sepharose Fast Flow chromatography, the unabsorbed fraction, termed as neutral polysaccharides (Fig. 1B), was further purified by Sephacryl S-500 HR chromatography. The major peak, appeared as single and symmetrical, was collected and lyophilized, named as RPS-1 (Fig. 1C). The HPSEC profile of RPS-1 showed a single and symmetrical sharp peak, indicating its homogeneity (Fig. 1D). The weight-average molecular weight (M_w) of RPS-1 was 1.617×10^7 Da and its z-average root mean square radius (RMS) was 27.5 nm (Table 1).

3.2. Physicochemical properties and structural feature of RPS-1

According to the data of MALLS, the slope of log(RMS radius)/log(M_w) plot was 0.15, less than 0.33 (Table 1), which indicated that RPS-1 existed as compact spherical conformations (Wyatt, 1993). To provide direct evidence of the chain conformation of RPS-1, molecular morphology of RPS-1 in water was observed by atomic force microscope imaging system (JPK, Germany). As shown in Supplementary Fig. 1, individual spherical particles were imaged clearly. However, the slow drying process of liquid samples prior to AFM analysis resulted in aggregation of polysaccharide molecules.

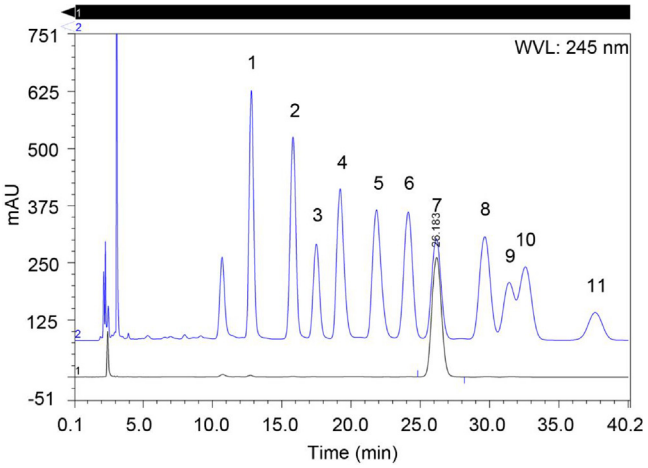

Fig. 2. Monosaccharide composition analysis of RPS-1. RPS-1 was hydrolyzed by 2.0 M trifluoroacetic acid (TFA) at 110 °C for 4 h and react with 0.5 M PMP. PMP derivatives of RPS-1 (black line) and monosaccharide standard samples (blue line) (1-Man, 2-GlcN, 3-Rha, 4-GlcA, 5-GalA, 6-GalN, 7-Glc, 8-Gal, 9-Xyl, 10-Ara and 11-Fuc) were analyzed by HPLC (UltiMate 3000) equipped with Kromasil C18 HPLC column (4.6 mm × 150 mm, 5 μm) and ultraviolet detector (For interpretation of the references to color in this figure legend, the reader is referred to the web version of this article).

RPS-1 showed negative reaction with iodine-iodide and had no absorption at 280 nm and 260 nm, which indicated the absence of starch-type polysaccharide, protein and nucleic acid. The total sugar content of RPS-1 was 99.28%. According to monosaccharide composition analysis, only one peak was observed and identified as glucose (Fig. 2). The IR spectrum of RPS-1 showed the characteristic peaks of polysaccharide at 3310.41, 2928.66 and 1652.04 cm^{-1} (Fig. 3). According to data of methylation analysis, the linkage types of RPS-1 contained Glc*p*-(1→, (1→4)-linked glucopyranosyl units and (1→4, 6)-linked glucopyranosyl units in the molar ratio of 6.9: 86.1: 6.9 (Supplementary Fig. 2 and Supplementary Table 1). Signals of RPS-1 in 1D NMR spectra were assigned on the basis of monosaccharide composition, linkage analysis, and chemical shift by comparing with previous studies in combination with the peak intensity (Synytsya & Novak, 2013). Only signals of α-D-glucan appeared in the anomeric region of both the ^1H (5.35 and 4.92 ppm) and ^{13}C NMR (99.86, 76.95, 69.43, 60.58 ppm) spectra, which indicated all of the residues are of α-configuration (Fig. 4).

From the aforementioned results, RPS-1 was deduced to be a glycogen-like polysaccharide consisting of a backbone structure of (1→4)-linked α-D-glucopyranosyl residues substituted at the O-6 position with α-D-glucopyranosyl branches on average 14.5 residues.

3.3. RPS-1 stimulated the production of NO and TNF-α in macrophages

Macrophages are key effector cells of the innate immune response to

Table 1
Experimental data of MALLS for RPS-1 in 0.2 mol/l sodium nitrate solution at 25 °C.

Molar mass ($\times 10^7$ Da)			Polydispersity index		RMS radius (nm)			Conformation plot slope
M_n	M_w	M_z	M_w/M_n	M_z/M_n	R_n	R_w	R_z	Log(radius)/log(M_w)
1.214	1.617	2.958	1.332	2.437	22.9	24.2	27.5	0.15

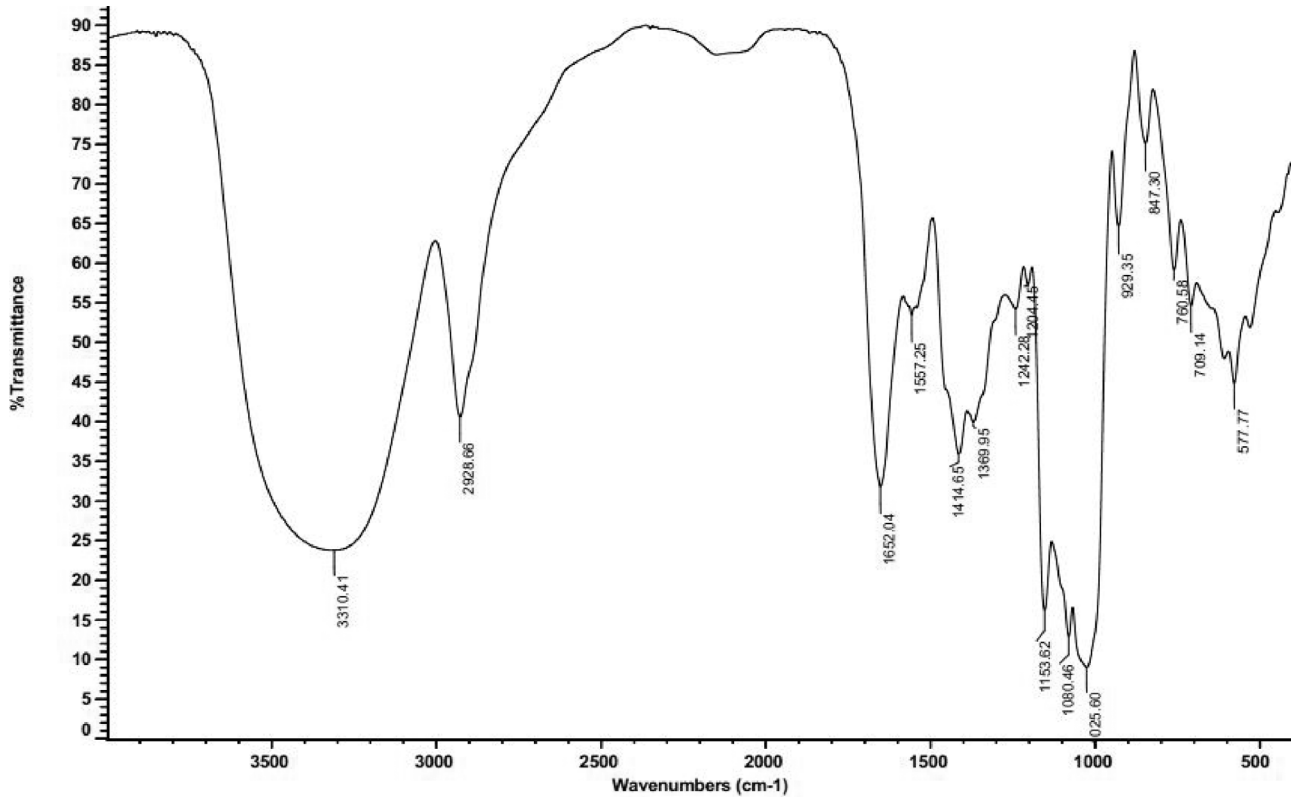

Fig. 3. Infrared spectrum analysis of RPS-1. The infrared spectrum of RPS-1 was recorded with a Nicolet Avatar 370 spectrometer (Nicolet, USA) in the range of 400–4000 cm^{-1}.

pathogen invasion and contribute to tumor destruction. They play important roles in the antigen presentation and clearance of pathogens and cancerous cells. Several studied have reported the immuno-enhancing activity and antitumor effect of natural and enzymatically synthesized (1→4)-α-glucan (Kakutani et al., 2012; Ryoyama, Kidachi, Yamaguchi, Kajiura, & Takata, 2004; Takaya et al., 1998). To explore the potential immunomodulatory activity of RPS-1, we studied the effects of RPS-1 on the activation of murine macrophages RAW 264.7 cells. Firstly, the cytotoxic effect on RAW 264.7 cells was analyzed by MTT assay and RPS-1 failed to show any cytotoxicity up to 1 mg/ml in vitro (data not shown). We detected the NO and TNF-α in RAW 264.7 cells challenged with RPS-1. As shown in Fig. 5, the release of TNF-α was significantly stimulated by RPS-1 from 50 to 400 μg/ml, whereas RPS-1 stimulated the production of NO only at high concentrations (200 and 400 μg/ml). To exclude the possible contamination of LPS in RPS-1, RAW 264.7 cells were pretreated with PMB, a specific inhibitor of LPS, followed by treatment with RPS-1 or LPS for 24 h. PMB could significantly blocked the production of NO and TNF-α induced by LPS, while pre-incubation with PMB only slightly attenuated RPS-1 induced cytokine and NO secretion (Supplementary Fig. 3). These results suggested that RPS-1 could activate murine macrophages RAW 264.7 cells.

3.4. RPS-1 activated MAPKs and NF-κB pathways in RAW 264.7 cells

There are three well-defined MAPK pathways: the extracellular-signal-regulated kinase (ERK) pathway, the JUN N-terminal kinase (JNK) pathway and the p38 pathway (Johnson & Lapadat, 2002). To investigate whether the MAPK pathways were involved in RPS-1 induced macrophage activation, we performed western blot analysis to detect the phosphorylation of MAPKs in RAW 264.7 cells. As shown in Fig. 6, upon challenged with RPS-1, the elevated phosphorylation of MAPKs appeared after 15 min and the maximal phosphorylation of p38 and JNK1/2 occurred at 15 min and 30 min, respectively. After that, the bands attenuated with prolonged incubation time. In LPS-activated macrophages, rapid phosphorylation of p38, JNK1/2 and ERK1/2 was observed in 5 min. The protein levels of phosphorylated active form of p38 and JNK gradually returned to the basal level after 30 min, whereas ERK1/2 phosphorylation was maintained at high level even after 60 min. In summary, RPS-1 induced phosphorylation of all three MAPKs in a time-dependent pattern which was different from LPS stimulation.

Further, to clarify whether RPS-1 could activate NF-κB pathway, the levels of IκBα and NF-κB p65 subunit were assessed in the cytosolic and nuclear fractions, respectively. After exposure to RPS-1 for 30 min, the red fluorescence of NF-κB p65 subunit was increased in nuclear regions compared with control group (Fig. 7A). Upon RPS-1 stimulation, a continuous reduction of IκBα in the cytosol and a concomitant increase of NF-κB p65 in the nucleus were noted, which indicated that RPS-1 induced nuclear translocation of NF-κB p65 (Fig. 7B). According to the data of luciferase reporter gene assay, a significantly increase of transcriptional activity of NF-κB was observed in RPS-1 treated group as well as in LPS stimulated group (Supplementary Fig. 4). These results indicated that RPS-1 induced nuclear translocation and activation of NF-κB in RAW 264.7 cells.

3.5. The roles of MAPKs and NF-κB pathways in macrophage activation induced by RPS-1

To confirm the roles of MAPKs and NF-κB signaling pathways in the secretion of NO and TNF-α induced by RPS-1, RAW 264.7 cells were preincubated with specific inhibitors for 1 h. As shown in Supplementary Fig. 5, production of NO and TNF-α induced by RPS-1 was almost completely inhibited by BAY 11-7082, inhibitor of NF-κB. The inhibitors of MAPKs could significantly weakened TNF-α release, whereas SP600125 and PD98059 approximately suppressed half of NO production. However, SB203580, inhibitor of phospho-p38, failed to

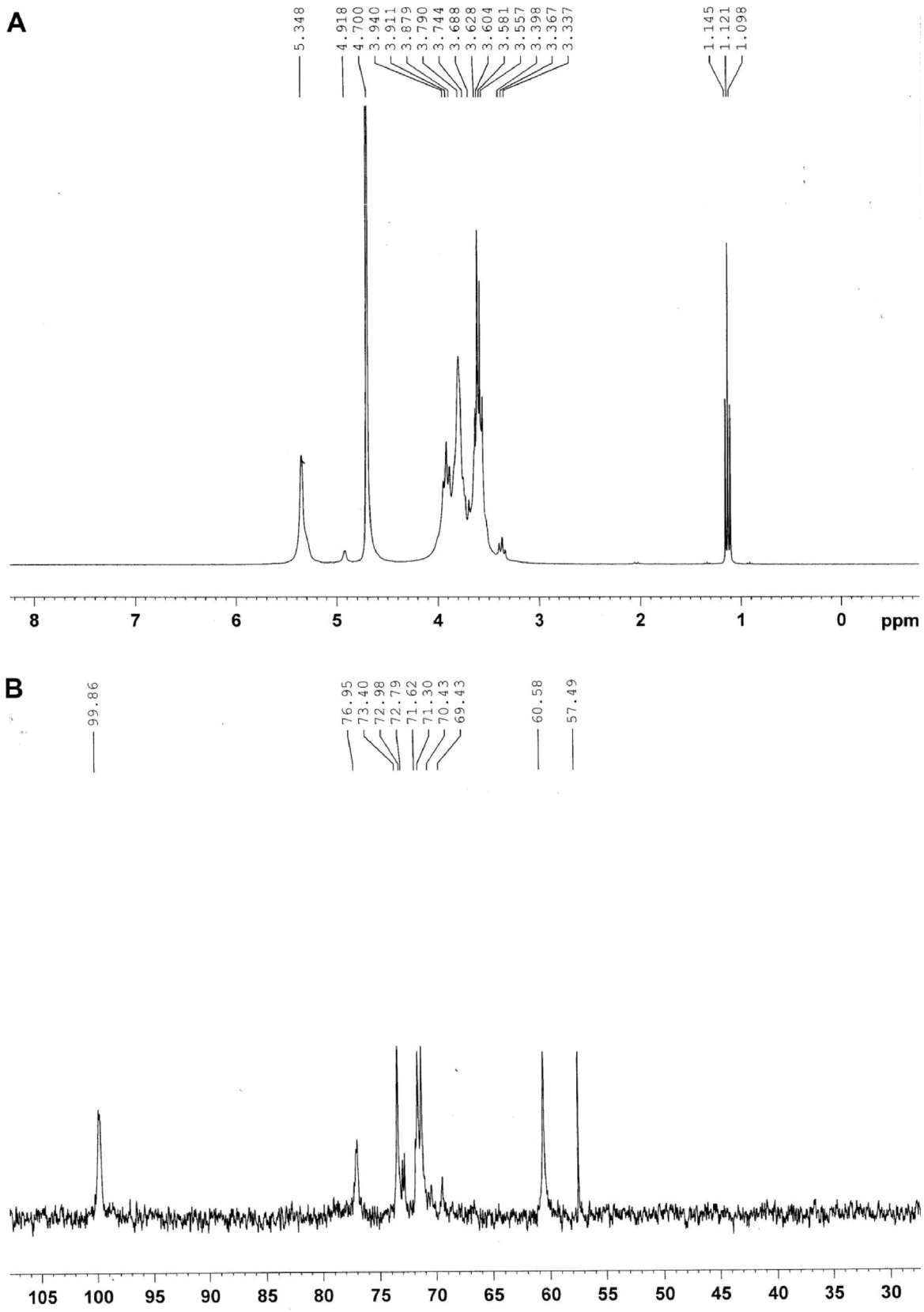

Fig. 4. ^{1}H and ^{13}C NMR spectra of RPS-1. A total of 10 mg of RPS-1 was dissolved in 0.5 ml of D_2O. (A) ^{1}H and (B) ^{13}C NMR spectra of RPS-1 were recorded on a Bruker AVANCE-300 MHz NMR spectrometer (Bruker, Germany) at 25 °C.

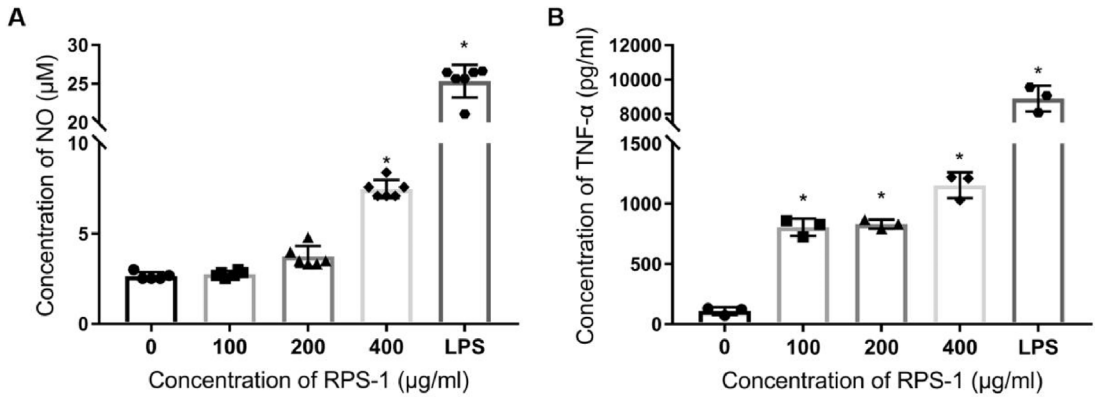

Fig. 5. RPS-1 stimulated the production of NO and TNF-α in RAW 264.7 cells. RAW 264.7 cells were treated with indicated concentrations of RPS-1 or LPS (100 ng/ml) for 24 h. Supernatant (A) NO and (B) TNF-α levels were detected by Griess reagent and ELISA, respectively. Results were expressed as mean values ± SD (n = 3 or n = 6, * $p \leq 0.05$ versus control group).

show inhibitory effect on the NO production induced by RPS-1 (Supplementary Fig. 5A), which suggested that distinct expression pattern of NO and TNF-α was involved in the activation of RAW 264.7 cells in response to RPS-1.

3.6. RPS-1 suppressed the tumor growth in CT26 tumor-bearing mice

The macrophage activation induced by RPS-1 in vitro prompted us to evaluate the antitumor and immunomodulatory properties in vivo. Whether polysaccharides display biological activity depends on the stable spatial configuration under physiological conditions (Masuda et al., 2017; Zhang et al., 2005). RPS-1 was characterized as α-(1→6)-branched α-(1→4)-glucan and the pancreatic α-amylase in small intestinal lumen may digest RPS-1 and impaired its potential immunoregulatory activity in vivo. Therefore, we tested the degradation of RPS-1 treated with pancreatic α-amylase by particle size analysis. As shown in Supplementary Fig. 6A, amylopectin from maize, highly-branched α-1,4 glucan with α-1,6 branch, was digested in several hours and further degraded at 12 h after treatment of pancreatic α-amylase. Under the same conditions, the average diameter of RPS-1 was slightly decreased until 12 h, from 59.31 nm to 56.25 nm (Supplementary Fig. 6B and Supplementary Table 2). These data suggest that RPS-1 was more resistant to pancreatic α-amylase than natural amylopectin. The compact globular molecular conformations might partially render RPS-1 resistant to α-amylase.

We established subcutaneous CT26 tumor-bearing model in BALB/c mice. After intragastric administration of RPS-1, the tumor growth of CT26 bearing mice was significantly inhibited in 200 mg/kg/day group and increased immune organ indexes were simultaneous observed in RPS-1 treatment group from 50 to 200 mg/kg/day (Table 2). We found that treatment of RPS-1 resulted in higher secretion of Th1 cytokines, including IL-2 and TNF-α, as well as immunoglobulin G in syngeneic tumor model (Fig. 8A–C). RPS-1 and 5-FU, alone and combination, tilted the balance of Bcl-2 and Bax towards proapoptosis functions in tumor tissues (Fig. 8D). Moreover, combined administration of RPS-1 (200 mg/kg/day) and 5-FU (20 mg/kg/day) showed stronger antitumor activity and partially alleviated immunosuppression induced by 5-FU (Table 2 and Fig. 8).

4. Discussion

For many years, harnessing the immune system to fight cancer is a promising approach for the majority of cancer patients (Couzin-Frankel, 2013). Natural fungal polysaccharides possess immunomodulatory activity and have been used to improve general health for decades in Asian countries, especially in combination with cytotoxic-chemotherapeutic agent for the treatment of cancers. In this study, we demonstrated that *R. nigricans* polysaccharide RPS-1, α-(1→6)-branched α-(1→4)-glucan, activated macrophage and significantly inhibited tumor growth in CT26 tumor-bearing mice.

Growing evidences have revealed the crucial role of structure in the bioactivity of polysaccharide (Li et al., 2016). Several structural features were involved in the structure-activity relationship of polysaccharide, including monosaccharide composition, molecular weight,

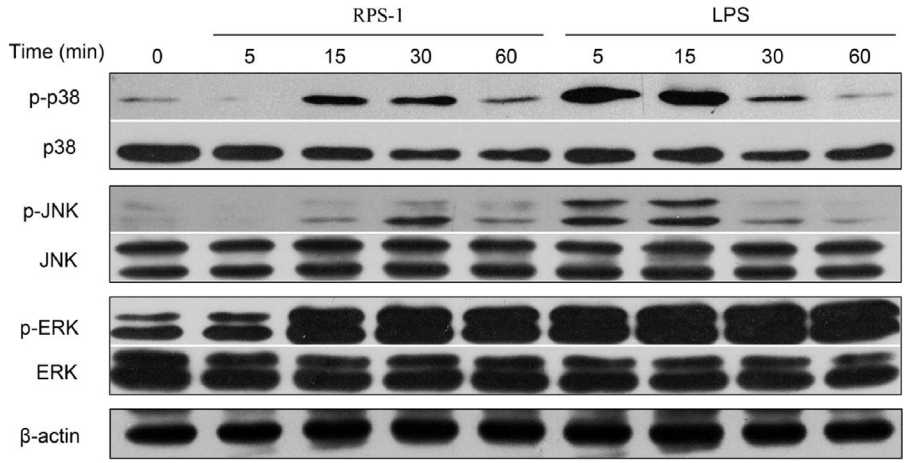

Fig. 6. RPS-1 induced phosphorylation of p38, JNK and ERK in RAW 264.7 cells. After treated with RPS-1 or LPS for indicated time, levels of protein expression were analyzed by western blot analysis.

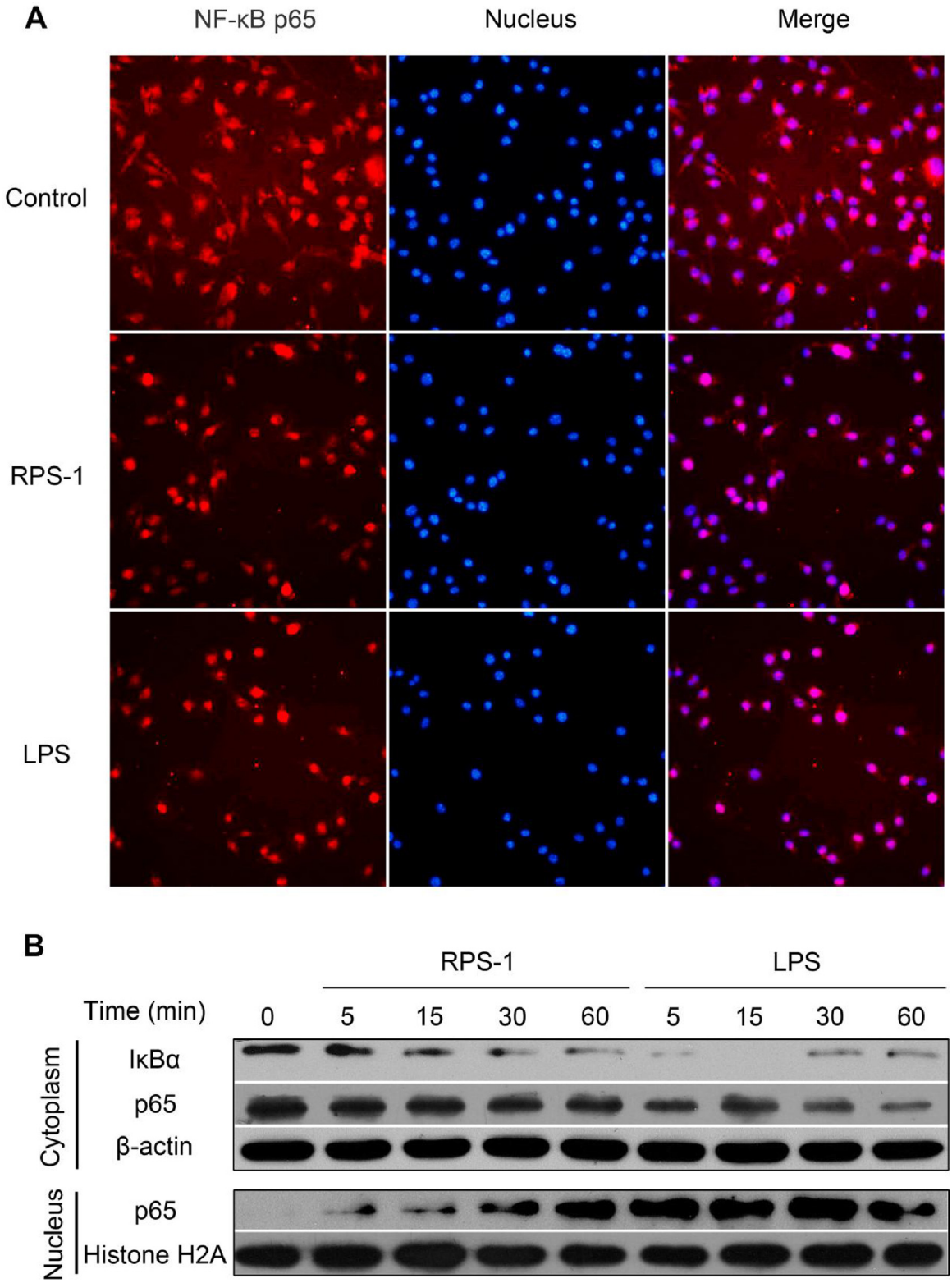

Fig. 7. RPS-1 induced nuclear translocation of NF-κB in RAW 264.7 cells. (A) After treated with RPS-1 (400 μg/ml) or LPS (100 ng/ml) for 30 min, cells were fixed and incubated with primary antibody against NF-κB p65 and Cy-3 conjugated secondary antibody. After stained with DAPI, the prepared samples were photographed by using fluorescence microscopy (Olympus, Japan). (B) RAW 264.7 cells were stimulated with RPS-1 or LPS for indicated time (5, 15, 30, 60 min) and nuclear and cytoplasmic extracts were prepared. Levels of protein expression of NF-κB p65 and IκBα were measured by western blot analysis.

glycosidic linkage types and the conformation. Thus, structure characteristics of RPS-1 were investigated to elucidate the basis of biological activity. The weight-average molecular weight of RPS-1 was estimated to be 1.617×10^7 Da and its R_Z was 27.5 nm (Fig. 1D and Table 1), which was similar to results reported from *Ostrea edulis* glycogen (Fernandez, Rojas, & Nilsson, 2011). RPS-1 was identified as a homogeneous water-soluble glucan consisting of (1→4)-linked α-D-Glc*p* residues and (1→4, 6) linked α-D-Glc*p* branches (Figs. 2 and 4). The fine

Table 2
Effects of RPS-1 on the body weight, immune organ index and tumor growth of CT26 tumor-bearing mice (n = 6, * $p \leq 0.05$ versus control group, $^{\#}$ $p \leq 0.05$ versus 5-FU group).

Group	Dosage mg/kg/day)	Body weight (g)	Spleen index (mg/g)	Thymus index (mg/g)	Tumor weight (g)
Control	–	23.69 ± 2.24	9.13 ± 2.02	4.37 ± 0.58	0.58 ± 0.13
RPS-1	50	24.14 ± 1.45	9.37 ± 0.89	4.86 ± 0.61	0.51 ± 0.15
	100	25.26 ± 0.67	10.18 ± 0.81	5.29 ± 0.62*	0.49 ± 0.14
	200	25.02 ± 1.12	9.18 ± 1.26	4.95 ± 0.63	0.33 ± 0.17*
5-FU	20	17.90 ± 2.95*	4.68 ± 1.38*	3.04 ± 0.69*	0.28 ± 0.12*
Combined treatment	200 (RPS-1) + 20 (5-FU)	19.39 ± 1.59*	6.15 ± 1.56*	3.99 ± 0.75$^{\#}$	0.16 ± 0.14*

structures of these macromolecules including branching degree, molecular weight and spatial structure play a key role in the physiological activities (Kakutani et al., 2007). A polysaccharide (YCP) possessed linear α-(1→4) bonded glucopyranoside main chain and α-(1→6) side chain from marine filamentous fungus *Phoma herbarum* YS4108 increased phagocytic activity of mice macrophages in vitro and in vivo (Yang et al., 2005). However, the fragments of YCP with different molecular weight showed different immunological activities and receptor signaling pathways (Ren, Yan, Yao, Jin, & Gao, 2010; Zhu et al., 2014). The lengths of backbone and side chains as well as branches are not known from this study and further research should be performed to ascertain the primary structure and spatial configuration of RPS-1 in physiological conditions.

Recently, some natural and enzymatically synthesized polysaccharides consisting of highly α-(1→6)-branched α-(1→4)-glucan backbone exhibit various physiological effects in vitro and vivo such as anticancer and immunoregulation (Masuda et al., 2017; Takaya et al., 1998). Response to biologically active polysaccharides, macrophage released a variety of inflammatory cytokines, chemokines and other immune-modulating mediators to modulate immune function and increased capacity to eliminate invading pathogens and tumor cells (Lee et al., 2015; Wang et al., 2014). RPS-1 promoted production of NO and TNF-α in RAW 264.7 murine macrophages in a concentration-dependent manner (Fig. 5) and pretreatment with PMB showed no obvious effects (Supplementary Fig. 3). MAPKs are a group of serine/threonine protein kinases and have an important role in variety cellular processes, such as proliferation, differentiation, apoptosis and immune defence. A number of immunomodulatory agents have been found to modulate both innate and adaptive immunity by influencing MAPK signaling cascade (Alamuru et al., 2014; Xu, Pan, Zhang, & Ashida, 2011). To

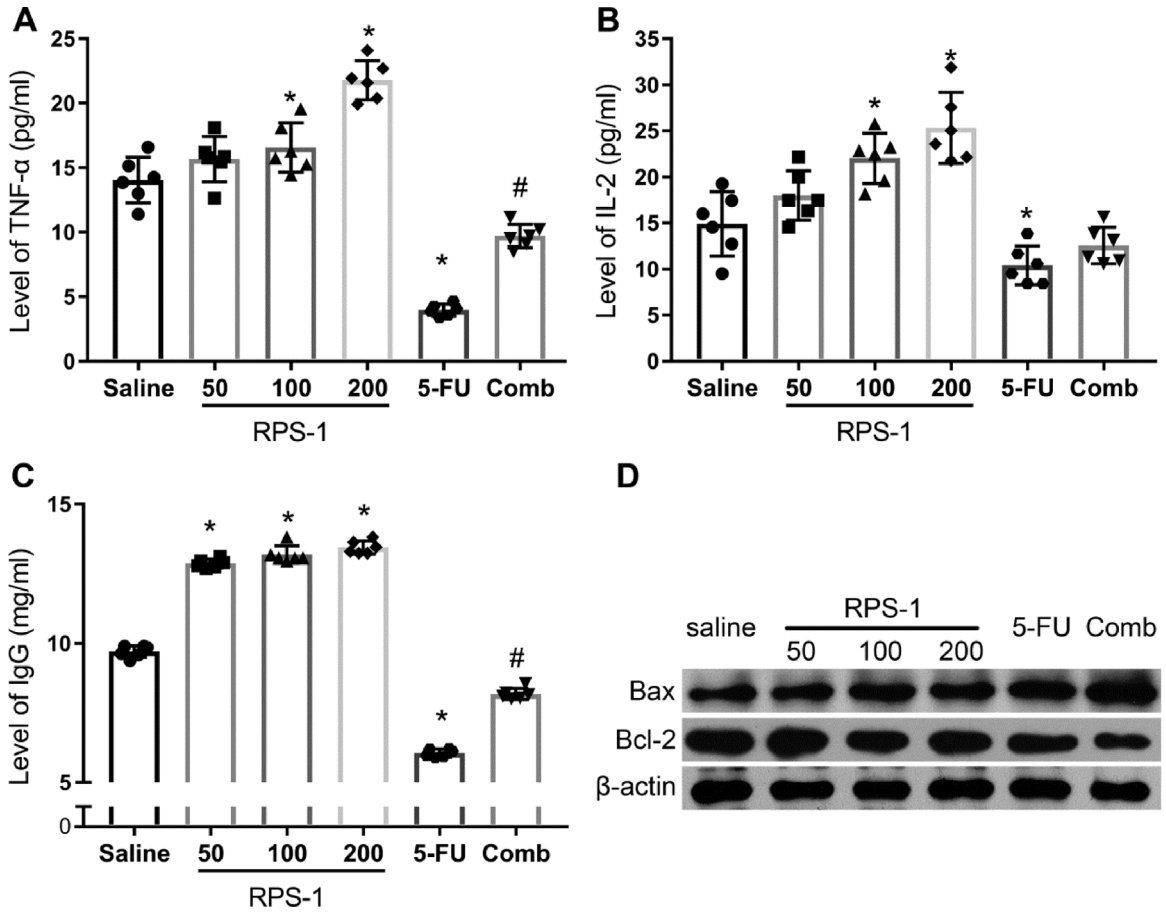

Fig. 8. Effects of RPS-1 on serum cytokines levels and apoptotic related proteins expression levels. At the end of the experiment, orbital sinus blood sample was collect and the concentrations of (A) TNF-α and (B) IL-2 were assayed by commercial ELISA kits (* $p \leq 0.05$ versus control group, # $p \leq 0.05$ versus 5-FU group). (C) Tumor tissue lysates were prepared and levels of protein expression were analyzed by western blot analysis. Comb: combined treatment.

explore the possible molecular mechanisms involved in the activation of macrophage induced by RPS-1, we detected the expression of proteins that are associated with MAPK signaling pathway. The elevated phosphorylation of MAPKs was observed after treated with RPS-1 for 15 min in RAW 264.7 cells (Fig. 6). The inhibitors of JNK and ERK significantly weakened NO and TNF-α release (Supplementary Fig. 5). However, inhibitor of phospho-p38, SB203580, had no influence on the NO production (Supplementary Fig. 5A). These results demonstrated that MAPKs and NF-κB signaling pathways participated in the production of NO and TNF-α induced by RPS-1.

In unstimulated cells, NF-κB is sequestered in the cell cytoplasm as an inactive protein complex by IκB family proteins (e.g., IκBα, IκBβ, and IκBε) (Ghosh, May, & Kopp, 1998). Response to external stimulus with a variety of agonists, inhibitor of nuclear factor kappa-B kinase (IKK) induced phosphorylation of IκBα leading to degradation via ubiquitination pathway (Karin & Ben-Neriah, 2000). It is now generally accepted that NF-κB signaling pathway participate in the expression of inflammatory cytokines and mediators in macrophage. The recognition of ligands by pattern recognition receptors on the cell surface or in the cytoplasm of innate immune cells initiates activation of MAPKs and NF-κB, leading to the expression of multiple genes that modulate the inflammatory response (Arthur & Ley, 2013; Hayden & Ghosh, 2004). Consistent with such a role, NF-κB is employed to manipulate the signal output of heterologous receptors of immune cells upon exposure to immunoregulatory polysaccharides (Chen et al., 2017). After treated with RPS-1, a continuous reduction of IκBα in the cytosol and a concomitant increase of NF-κB p65 in the nucleus were noted (Fig. 7A and B). Consistent with this, RPS-1 significantly increased transcriptional activity of NF-κB (Supplementary Fig. 4).

Macrophages play an important role in innate and adaptive immune responses and are responsible for immunoregulatory activity of bioactive polysaccharides. In recent decades, immunoregulatory polysaccharides have attracted a great deal of attention in oncotherapy because of their potent therapeutic effect against malignant tumors and relatively low toxicity. Maitake α-glucan derived from *Grifola frondosa* activated macrophages and dendritic cells, and stimulated the synthesis of cytokines and chemokines to modulate the antitumor immune response (Ngo et al., 2015). In our study, intragastric consumption of RPS-1 alone or plus 5-FU significantly delayed the tumor growth in CT26 tumor-bearing mice (Table 2). We found that RPS-1 did not show tumoricidal activity in vitro, but increased immune organ index and secretion of Th1 cytokines (TNF-α and IL-2) and IgG in syngeneic tumor model (Table 2 and Fig. 8), which should stimulate antitumor cytotoxic T lymphocyte and antibody depend tumoricidal activity. IL-2 could mediate differentiation of $CD8^+$ into memory and more terminally differentiated effector phenotypes, subsequently primed antitumor T-cell responses, and has been proved as one effective immunotherapy for patients with solid cancer (IL-2: The First Effective Immunotherapy for Human Cancer). In combination with 5-FU, RPS-1 displayed enhancing and alleviated 5-FU induced immunosuppression (Table 2 and Fig. 8). These data suggest that intragastric administration of RPS-1 was effective against colon cancer and improved immunosuppression and toxicity induced by 5-FU in tumor-bearing mice. The bridges between macrophage activation and tumor regression induced by RPS-1 remained unclear. Further studies are required to explore the immune cell dynamics in gut-associated lymphoid tissue and intratumoral region during RPS-1 treatment.

In summary, we described the purification and characterization of a novel polysaccharide isolated from liquid-cultured mycelia of *R. nigricans* and our data provide evidence that RPS-1 stimulated production of NO and TNF-α through MAPKs and NF-κB signaling pathways in macrophage RAW 264.7 cell line. Moreover, intragastric administration of RPS-1 significantly delayed tumor growth and enhanced the effectiveness of chemotherapy. These findings would be beneficial for the discovery of RPS-1 as dietary supplements and functional foods.

Conflict of interest statement

The authors have declared no conflict of interest.

Acknowledgements

This study was supported by Major Projects from the Science and Technology Program of Shandong Province (the Key Technology) (No. 2015ZDJS04002), the Major State Basic Research Development Program of China (973 Program) (No. 2012CB822102), the High Technology Research and Development Program of China (863 Program) (No. 2012AA021501), National Natural Science Foundation of China (NSFC) (No. 81702581) and the Scientific and Technological Innovation Commission of Shenzhen (No. JCYJ20170306091400043).

Appendix A. Supplementary data

Supplementary material related to this article can be found, in the online version, at doi:https://doi.org/10.1016/j.carbpol.2018.06.076.

References

Alamuru, N. P., Behera, S., Butchar, J. P., Tridandapani, S., Suraj, S. K., Babu, P. P., et al. (2014). A novel immunomodulatory function of PHLPP1: Inhibition of iNOS via attenuation of STAT1 ser^{727} phosphorylation in mouse macrophages. *Journal of Leukocyte Biology, 95*, 775–783.

Arthur, J. S., & Ley, S. C. (2013). Mitogen-activated protein kinases in innate immunity. *Nature Reviews Immunology, 13*, 679–692.

Brown, G. D., & Gordon, S. (2001). Immune recognition – A new receptor for beta-glucans. *Nature, 413*, 36–37.

Chen, G. C., Zhang, P. Y., Huang, T. T., Yu, W. Q., Lin, J., Li, P., et al. (2013). Polysaccharides from *Rhizopus nigricans* mycelia induced apoptosis and G2/M arrest in BGC-823 cells. *Carbohydrate Polymers, 97*, 800–808.

Chen, S., Yin, D. K., Yao, W. B., Wang, Y. D., Zhang, Y. R., & Gao, X. D. (2009). Macrophage receptors of polysaccharide isolated from a marine filamentous fungus *Phoma herbarum* YS4108. *Acta Pharmacologica Sinica, 30*, 1008–1014.

Chen, Y. N., Li, H. F., Li, M. F., Niu, S. B., Wang, J. X., Shao, H. W., et al. (2017). *Salvia miltiorrhiza* polysaccharide activates T lymphocytes of cancer patients through activation of TLRs mediated -MAPK and -NF-kappa B signaling pathways. *Journal of Ethnopharmacology, 200*, 165–173.

Ciucanu, I., & Kerek, F. (1984). A simple and rapid method for the permethylation of carbohydrates. *Carbohydrate Research, 131*, 209–217.

Couzin-Frankel, J. (2013). Cancer immunotherapy. *Science, 342*, 1432–1433.

Fernandez, C., Rojas, C. C., & Nilsson, L. (2011). Size, structure and scaling relationships in glycogen from various sources investigated with asymmetrical flow field-flow fractionation and H-1 NMR. *International Journal of Biological Macromolecules, 49*, 458–465.

Gantner, B. N., Simmons, R. M., Canavera, S. J., Akira, S., & Underhill, D. M. (2003). Collaborative induction of inflammatory responses by dectin-1 and toll-like receptor 2. *Journal of Experimental Medicine, 197*, 1107–1117.

Ghosh, S., May, M. J., & Kopp, E. B. (1998). NF-kappa B and Rel proteins: Evolutionarily conserved mediators of immune responses. *Annual Review of Immunology, 16*, 225–260.

Hayden, M. S., & Ghosh, S. (2004). Signaling to NF-kappaB. *Genes & Development, 18*, 2195–2224.

Ina, K., Kataoka, T., & Ando, T. (2013). The use of lentinan for treating gastric cancer. *Anti-Cancer Agents in Medicinal Chemistry, 13*, 681–688.

Johnson, G. L., & Lapadat, R. (2002). Mitogen-activated protein kinase pathways mediated by ERK, JNK, and p38 protein kinases. *Science, 298*, 1911–1912.

Kakutani, R., Adachi, Y., Kajiura, H., Takata, H., Kuriki, T., & Ohno, N. (2007). Relationship between structure and immuno stimulating activity of enzymatically synthesized glycogen. *Carbohydrate Research, 342*, 2371–2379.

Kakutani, R., Adachi, Y., Kajiura, H., Takata, H., Kuriki, T., & Ohno, N. (2012). The effect of orally administered glycogen on anti-tumor activity and natural killer cell activity in mice. *International Immunopharmacology, 12*, 80–87.

Karin, M., & Ben-Neriah, Y. (2000). Phosphorylation meets ubiquitination: The control of NF-kappaB activity. *Annual Review of Immunology, 18*, 621–663.

Lee, J. S., Kwon, D. S., Lee, K. R., Park, J. M., Ha, S. J., & Hong, E. K. (2015). Mechanism of macrophage activation induced by polysaccharide from *Cordyceps militaris* culture broth. *Carbohydrate Polymers, 120*, 29–37.

Li, S. J., Xiong, Q. P., Lai, X. P., Li, X., Wan, M., Zhang, J. N., et al. (2016). Molecular modification of polysaccharides and resulting bioactivities. *Comprehensive Reviews in Food Science and Food Safety, 15*, 237–250.

Long, K. B., & Beatty, G. L. (2013). Harnessing the antitumor potential of macrophages for cancer immunotherapy. *Oncoimmunology, 2*, e26860.

Masuda, Y., Nakayama, Y., Tanaka, A., Naito, K., & Konishi, M. (2017). Antitumor activity of orally administered maitake alpha-glucan by stimulating antitumor immune response in murine tumor. *PLoS One, 12*, e0173621.

Namikawa, T., Fukudome, I., Ogawa, M., Munekage, E., Munekage, M., Shiga, M., et al.

(2015). Clinical efficacy of protein-bound polysaccharide K in patients with gastric cancer undergoing chemotherapy with an oral fluoropyrimidine (S-1). *European Journal of Surgical Oncology, 41*, 795–800.
Ngo, D. H., Vo, T. S., Ngo, D. N., Kang, K. H., Je, J. Y., Pham, H. N. D., et al. (2015). Biological effects of chitosan and its derivatives. *Food Hydrocolloids, 51*, 200–216.
Ren, M., Yan, W., Yao, W. B., Jin, L., & Gao, X. D. (2010). Enzymatic degradation products from a marine polysaccharide YCP with different immunological activity and binding affinity to macrophages, hydrolyzed by alpha-amylases from different origins. *Biochimie, 92*, 411–417.
Ryoyama, K., Kidachi, Y., Yamaguchi, H., Kajiura, H., & Takata, H. (2004). Anti-tumor activity of an enzymatically synthesized alpha-1,6 branched alpha-1,4-glucan, glycogen. *Bioscience, Biotechnology, and Biochemistry, 68*, 2332–2340.
Sevag, M. G. (1938). The presence of a type-and species-specific conjugated polysaccharide in type I *Pneumococcus*. *Science, 87*, 304–305.
Sun, K. L., Chen, Y., Niu, Q. F., Zhu, W. M., Wang, B., Li, P. P., et al. (2016). An exopolysaccharide isolated from a coral-associated fungus and its sulfated derivative activates macrophages. *International Journal of Biological Macromolecules, 82*, 387–394.
Synytsya, A., & Novak, M. (2013). Structural diversity of fungal glucans. *Carbohydrate Polymers, 92*, 792–809.
Takaya, Y., Uchisawa, H., Ichinohe, H., Sasaki, J., Ishida, K., & Matsue, H. (1998). Antitumor glycogen from scallops and the interrelationship of structure and antitumor activity. *Journal of Marine Biotechnology, 6*, 208–213.
Thornton, B. P., Vetvicka, V., Pitman, M., Goldman, R. C., & Ross, G. D. (1996). Analysis of the sugar specificity and molecular location of the beta-glucan-binding lectin site of complement receptor type 3 (CD11b/CD18). *Journal of Immunology, 156*, 1235–1246.
Wang, J. Q., Nie, S. P., Cui, S. W., Wang, Z. J., Phillips, A. O., Phillips, G. O., et al. (2017). Structural characterization and immunostimulatory activity of a glucan from natural *Cordyceps sinensis*. *Food Hydrocolloids, 67*, 139–147.
Wang, L., Nie, Z. K., Zhou, Q., Zhang, J. L., Yin, J. J., Xu, W., et al. (2014). Antitumor efficacy in H22 tumor bearing mice and immunoregulatory activity on RAW 264.7 macrophages of polysaccharides from *Talinum triangulare*. *Food & Function, 5*, 2183–2193.
Wyatt, P. J. (1993). Light-scattering and the absolute characterization of macromolecules. *Analytica Chimica Acta, 272*, 1–40.
Wasser, S. P. (2010). Medicinal mushroom science: History, current status, future trends, and unsolved problems. *International Journal of Medicinal Mushrooms, 12*, 1–16.
Xu, X., Pan, C., Zhang, L., & Ashida, H. (2011). Immunomodulatory beta-glucan from *Lentinus edodes* activates mitogen-activated protein kinases and nuclear factor-kappaB in murine RAW 264.7 macrophages. *Journal of Biological Chemistry, 286*, 31194–31198.
Yang, X. B., Gao, X. D., Han, F., Xu, B. S., Song, Y. C., & Tan, R. X. (2005). Purification, characterization and enzymatic degradation of YCP, a polysaccharide from marine filamentous fungus *Phoma herbarum* YS4108. *Biochimie, 87*, 747–754.
Yu, Y., Shen, M. Y., Song, Q. Q., & Xie, J. H. (2018). Biological activities and pharmaceutical applications of polysaccharide from natural resources: A review. *Carbohydrate Polymers, 183*, 91–101.
Zhang, L., Li, X. L., Xu, X. J., & Zeng, F. B. (2005). Correlation between antitumor activity, molecular weight, and conformation of lentinan. *Carbohydrate Research, 340*, 1515–1521.
Zhu, R., Zhang, X., Liu, W., Zhou, Y., Ding, R., Yao, W. B., et al. (2014). Preparation and immunomodulating activities of a library of low-molecular-weight alpha-glucans. *Carbohydrate Polymers, 111*, 744–752.